THE ASTROPHYSICAL JOURNAL, 233:987–997, 1979 November 1

NUMERICAL MODELING OF QUASI-STATIC CORONAL LOOPS. I. UNIFORM ENERGY INPUT

J. F. VESECKY
Stanford Center for Radar Astronomy, Stanford University
AND
S. K. ANTIOCHOS AND J. H. UNDERWOOD
Institute for Plasma Research and Department of Applied Physics, Stanford University
Received 1978 November 6; accepted 1979 May 17

ABSTRACT

In closed, magnetic field regions of the solar corona the plasma is largely confined in loop or archlike structures of enhanced density; such features are easily seen on X-ray or EUV images of the corona. During a large part of their lifetimes these loops undergo no striking changes in either brightness or structure; hence a quasi-static (steady-state) model, balancing energy input to each volume element with radiative losses, and losses or gains by conduction, is appropriate. Quasi-static models have been investigated analytically by several authors. Our treatment is numerical so that we can include: gravity; an energy input function that is dependent on density, temperature, etc.; an accurate form for the radiative losses; and a variable cross-sectional area for the loop geometry. In this paper we consider a uniform energy input ϵ (per unit volume) and a variety of loop geometries presenting results for the run of electron density (n) and temperature (T) along the loop and the variation of differential emission measure with T, $\xi(T)$. X-ray images are presented showing significant variations of loop cross-sectional area along the loop length. Using a line dipole magnetic field model, we parametrize such area variations by Γ, the ratio between the cross-sectional area at the loop apex and at the base. Numerical modeling of coronal loops with $\Gamma > 1$ shows that loop temperature and density structure are relatively weak functions of Γ. However, these variations in n and T act in a cumulative fashion, making $\xi(T)$ a strong function of Γ near the loop apex. Thus, for a given loop, increases in Γ cause substantial increases in the amount of material at coronal temperatures ($\gtrsim 5 \times 10^5$ K). For the examples studied, changes in energy input cause roughly proportional changes in radiated power (loop brightness as observed in EUV or X-rays), but only small variations in maximum temperature. Observational experience at X-ray wavelengths reflect this result in that the corona over active regions varies in brightness, but seems always to have temperatures near 2 or 3×10^6 K. In our consideration of the general properties of quasi-static, coronal loop models we are led to several conclusions radically different from previous work. For a symmetrical loop, we argue that a symmetrical displacement of temperature maxima away from the loop apex does not, per se, make the top of the loop unstable—a perturbation analysis is necessary to determine the stability. Hence we conclude that even a symmetrical loop may, in general, have temperature maxima away from the apex.

Subject headings: plasmas — Sun: corona — Sun: flares

I. INTRODUCTION

Recent observations, in particular high-resolution X-ray and extreme-ultraviolet photographs of the Sun taken during the 1973–1974 *Skylab* missions, have revealed a wealth of structure in the solar corona. This structure is evidently determined by the coronal magnetic field. Where the field lines are open, the plasma may escape into interplanetary space and the density is reduced; a "coronal hole" results. In closed field regions, the plasma is confined into loop or archlike structures of enhanced density; such features are readily seen on X-ray photographs (Vaiana *et al.* 1973; Underwood *et al.* 1974). Most of the corona is organized into such loop structures, although they are brightest and most striking over centers of activity. It is apparent that future theoretical investigations of the heating and energy balance of the solar corona in both "quiet" and "active" regions must take this loop and arch structure into account.

Several models of coronal loop structures have been proposed. This paper is concerned with one of these—the "quasi-static" model. The model is designed to describe loops during the large part of their lifetime when they do not undergo striking changes in either structure or brightness (Gerassimenko, Solodyna, and Nolte 1978; Rosner, Tucker, and Vaiana 1978, p. 651 and references thereon). Hence, a *net* mass flow into or out of the loop during this time must be negligible. Since the lifetime of loops is frequently greater than

typical time scales for the loss of energy by radiation or conduction, a continuous input of energy must be assumed. Thus we are led to a steady-state model in which the mechanical energy deposited into each volume element is exactly balanced by radiative loss flux (F_R) and by conductive energy flux (F_c) into (or out of) the element (see Fig. 2). Since energy or mass transport across the loop is strongly inhibited by the magnetic field, the conduction is assumed to take place only along the field lines, i.e., along the length of the loop. We note here that in quasi-static models movements of the plasma (such as observed by Sandlin, Brueckner, and Tousey 1977; Nicolas *et al.* 1977; and Brueckner and Bartoe [1978] in the transition region) are not taken into account.

II. QUASI-STATIC CORONAL LOOPS

a) The Model

Rosner, Tucker, and Vaiana (1978) and Craig, McClymont, and Underwood (1978) have independently discussed the quasi-static loop model. Our treatment differs from these in that it is numerical rather than analytic. Hence we can include: gravity; an energy input function that is dependent on density, temperature, and position; an accurate form for the radiative losses; and a variable cross-sectional area for the loop geometry. The reason for assuming such a geometry is twofold. First, X-ray photographs show that loops of variable cross-sectional area, wider at the top than at the footpoints, occur frequently. Several examples are presented in Figure 1. Although many loops do appear to have constant cross-sectional area, it is possible that in many cases the finite resolution of the telescope obscures any area variation. Second, the field lines from a bipolar active region will diverge, and so the plasma contained by them would be expected to assume the shape of a loop of variable area. Such a variable area is likely to have a profound effect on the energy balance of the loop, in particular on the conduction term. This effect has been investigated, for the case of postflare loop cooling, by Antiochos and Sturrock (1976).

The model presented here assumes a loop configuration which, although simplified, represents approximately that to be expected from plasma confined by the field of a bipolar active region. Figure 2 depicts the adopted field configuration. A line dipole, buried at a depth d below the chromosphere (30,000 K level), is assumed to give rise to the observed photospheric fields and their potential extrapolation into the corona. We consider loops of height h, measured vertically from the dipole to the apex of the loop. The coordinate s is measured along $\boldsymbol{B}$ upward from the dipole origin. The loop structure of Figure 2 is taken to be a circular cylinder of varying radius (r) where r is perpendicular to the field line (which defines the axis of the loop) and is small compared with the loop length l. Thus in Figure 2 $dV = Ads = \pi r^2 ds$. If the loop's cross-sectional area $A(s)$ at a footpoint (i.e., at the chromospheric 30,000 K level) is a, then the area of the cross-section at the apex is Γa, where

$$\Gamma = h/d\,, \tag{1}$$

and the total length l of the loop, from footpoint to footpoint via the apex, is given by

$$l = 2h \cos^{-1}(\Gamma^{-1/2})\,. \tag{2}$$

These relations are somewhat different if the source is assumed to be a point dipole (see Antiochos and Sturrock 1976). However, the difference has little effect on the main conclusions of this study. The line dipole is perhaps most appropriate for those bipolar active regions in which the $\boldsymbol{B}$ fields are extended along the neutral line, causing the coronal loops to form arcades.

The energy balance of the loop is described by the equation

$$\nabla \cdot F_c = \epsilon - E_R\,, \tag{3}$$

where F_c is the conductive flux along the loop, ϵ the energy input, and E_R the radiative energy loss per cubic centimeter.

Because the conductive flux is essentially along the magnetic field line, equation (3) simplifies to the one-dimensional case:

$$\frac{1}{A(s)} \frac{d}{ds}\left[A(s)\kappa \frac{dT}{ds}\right] = n^2 \Lambda(T) - \epsilon\,. \tag{4}$$

In this equation, $A(s)$ represents the variation of cross-sectional area along the length of the loop, κ is the classical thermal conductivity, n is electron density, and $\Lambda(T)$ is the radiative loss function (computed, e.g., by Raymond, Cox, and Smith 1976). The plasma is also assumed to be in hydrostatic equilibrium, subject to the simplified force equation

$$\frac{dp}{ds} = \rho g_{\parallel}\,, \tag{5}$$

where $g_{\parallel}$ is the component of gravity parallel to $\boldsymbol{B}$. A numerical code, described in § III, was written to solve these equations for different loop geometries and assumed variations of energy input along the loop.

b) Boundary Conditions

The solution of equation (4) requires the specification of boundary conditions at both the top and the bottom of the loop. We assume that at the loop apex the conducted heat flux F_c is zero; this condition follows directly from the assumption of symmetry (see § IIc).

We assume also that F_c vanishes at some chromospheric level where the temperature is of the order of 10^4 K, or at least that it becomes very small compared with the value of F_c in the corona at $\sim 10^6$ K. This boundary condition was also assumed by Rosner *et al.* although they did not justify it. However, it can be seen to be a reasonable assumption through the following argument.

1979ApJ...233..987V

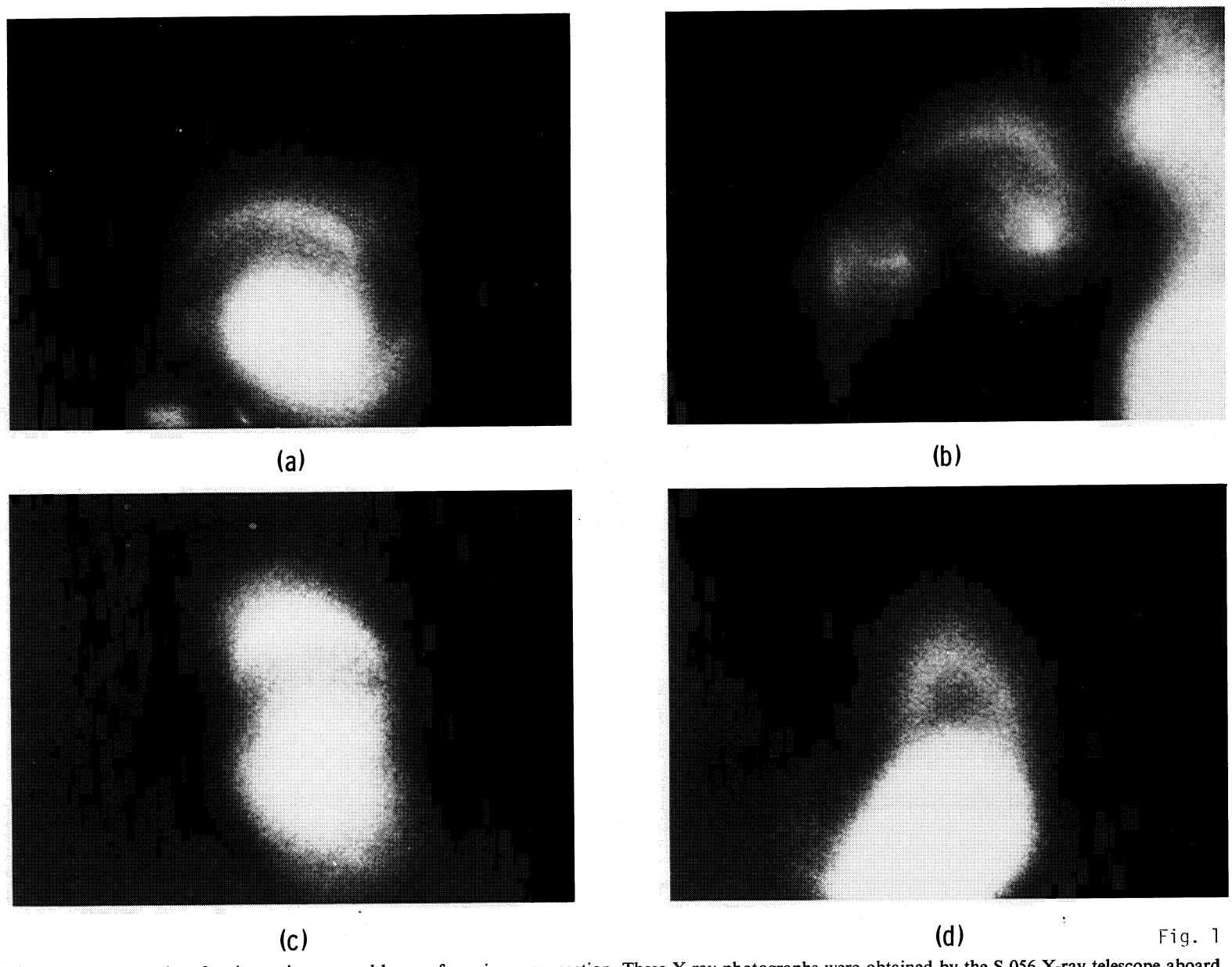

Fig. 1

FIG. 1.—Examples of active region coronal loops of varying cross section. These X-ray photographs were obtained by the S-056 X-ray telescope aboard *Skylab*. (*a*) 1973 Sep 4, 1602 UT; (*b*) 1973 Sep 4, 2233 UT; (*c*) 1973 Sep 7, 1417 UT; (*d*) 1974 Jan 22, 2331 UT.

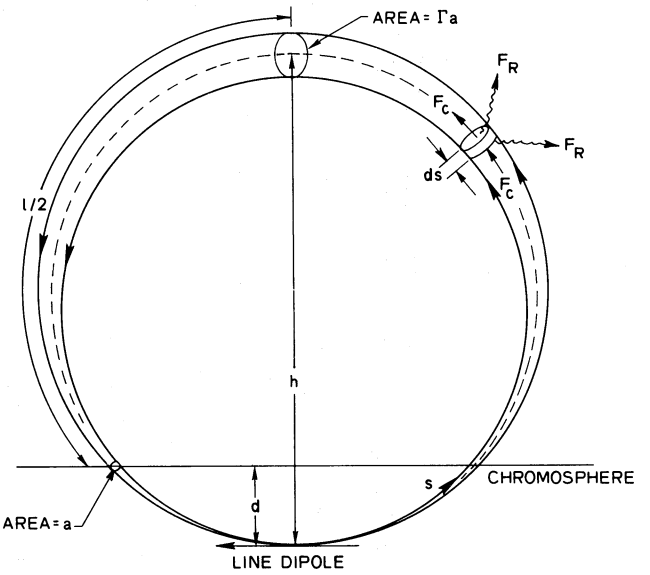

FIG. 2.—Coronal loop geometry for line dipole magnetic field. The origin of the line dipole is located at a depth d below the loop base (taken to be at the 30,000 K level in the upper chromosphere). The area factor Γ is defined as the ratio of the loop cross-sectional area at the apex to that at the base. The coordinate s is along the magnetic field line. A volume element dV having dimension ds along the magnetic field is shown with radiative (F_R) and convective fluxes (F_c) indicated schematically.

If the downward heat flux is to be dissipated by radiation, then we show below that the conductive flux at the base of the transition region must be small compared with that in the corona. Consider the ratio $R(T)$ of the change in the heat flux, $\Delta F_c(T)$, due to energy radiated from plasma in a logarithmic temperature interval about T, to the conductive flux $F_c(T)$. This is given by (see Antiochos and Sturrock 1978)

$$R(T) \equiv \frac{\Delta F_c(T)}{F_c(T)} = \frac{-n_e^2 \Lambda(T) H(T)}{F_c(T)}, \qquad (6)$$

where $H(T)$ is the scale length for temperature variation, defined as

$$H(T) = \left| \frac{1}{T} \frac{dT}{ds} \right|^{-1}, \qquad (7)$$

since

$$F_c(T) = -\kappa \frac{dT}{ds}, \qquad (8)$$

we obtain

$$H(T) = \frac{\kappa T}{|F_c(T)|}. \qquad (9)$$

Hence, using the Spitzer (1962) value for the conductivity, we obtain

$$H(T) \approx 10^{-6} T^{7/2} |F_c(T)|^{-1}. \qquad (10)$$

Substituting into equation (6) and assuming constant pressure, we obtain:

$$R(T) \propto \frac{-\Lambda(T) T^{3/2}}{F_c^2(T)}. \qquad (11)$$

Below $T \approx 10^6$ K, $\Lambda(T)$ varies, on the average, as a small negative power of T (see Table 1). For the purposes of this argument, we may assume $\Lambda(T) =$ constant.

The proof of our assertions now follows directly from proportionality (11). This formula implies that if at some temperature T_1 the radiative losses are negligible compared to the conductive flux [$R(T_1) \ll 1$], then the losses at all lower temperatures are also negligible [$R(T) \ll 1$] for all $T \leq T_1$. In particular, suppose that $R(T) \ll 1$ in the corona so that the heat flux through the corona is approximately constant. We note from proportionality (11) that for constant F_c, R *decreases* as T decreases, $R(T) \propto T^{3/2}$. Thus, if the coronal losses are negligible, the radiation from cooler material (e.g., the transition region), is even less significant. At first, this result appears surprising because the radiative losses per unit volume, $n^2\Lambda(T)$, actually increase as T decreases. The key point is that, although cooler material is a more effective radiator, there is much less of it; since, for constant heat flux, the temperature scale height decreases very rapidly as the temperature decreases (see eq. [10]).

From the argument above we conclude that a purely static model in which a downward (conductive) heat flux is ultimately dissipated by radiation is not consistent with a value of $R(T) \ll 1$ at any temperature in the model. If such a value occurs, then the heat flux at that point can never be radiated away. Note that this argument is not affected by the energy input, since that is only a heat source and cannot act to dissipate the heat flux (what is needed to invalidate this argument is a heat sink other than radiation). Of course, it is possible to construct mathematical coronal loop models in which $R(T) \ll 1$, so that a large heat flux occurs at the base of the transition region, and

then to simply postulate that the chromosphere can somehow dissipate this flux. However, our argument implies that such models are *not* consistent with a static chromospheric model in which radiation is the only cooling mechanism. Although the chromosphere may not explicitly appear in models with $R(T) \ll 1$, they implicitly assume that the heat flux out their base is balanced by some anomalous mechanism, e.g., mass motions.

Therefore, in order to have a truly static model, we conclude that R must be of order unity throughout the loop. In this case the heat flux is not constant and a significant fraction of the flux at any temperature is radiated away by the plasma at that temperature. From proportionality (11), we note that $R(T) \approx 1$ implies

$$F_c(T) \propto T^{3/4} . \tag{12}$$

Hence, the flux at the base of our model must be approximately one and one-half orders of magnitude smaller than its coronal value. In addition, we note that the radiative flux must also be maximum in the corona. The common view, that the bulk of the energy is conducted down from the corona to the transition region from whence it is radiated, is thus seen to be a misconception. The numerical results of Figure 3 confirm this statement; we find, by integrating the radiative energy flux per unit length, that the "coronal" portion (top 90%) of the loop where $1.4 \times 10^6 \leq T \leq 2.2 \times 10^6$ K radiates away some 43% of the total power deposited in the loop.

Also, since $R(T) \approx 1$ in the corona, the radiative flux there must be approximately equal to the conductive flux,

$$F_R \approx F_c . \tag{13}$$

This result has been obtained by other authors, e.g., Rosner *et al.* and Craig *et al.* The discussion above shows that this result follows directly from the requirement that the heat flux vanish at the base of our model.

The concept of the quasi-static state follows quite naturally from the assumption that all the energy is radiated away above the chromosphere. Suppose a loop is in quasi-static state and the energy input is suddenly increased. The coronal plasma will be insufficiently dense to radiate this extra energy away and will increase in temperature. This will lead in turn to an increased conductive flux on the lower layers. In order to remove this flux, an "anomalous" transport of energy must ensue; the "evaporation" mechanism, mentioned by Pye *et al.* (1978) and described by Antiochos and Sturrock (1978) in connection with the cooling of flare plasmas, provides such a process. Plasma will flow upward into the loop, increasing the density until once more the energy is radiated away above the chromospheric level. In the case of a *decrease* in energy input, the reverse process will occur; now the plasma is radiating too much energy and will cool rapidly, become radiatively unstable, and fall toward the chromosphere. The subsequent reduction in density will allow the quasi-static state to be established once more. While this argument explains the existence of the quasi-static state, the question of its stability in a particular instance can be answered only by a detailed perturbation analysis.

It should be noted that in the case of the upward evaporation of material the velocities are subsonic (Antiochos and Sturrock 1978), whereas the velocity of downward-condensing material may become supersonic (Antiochos 1976; Antiochos and Krall 1979). This may explain why predominantly downward velocities are observed in the transition region (see Pneuman and Kopp 1978).

c) *Loop Geometry, Thermal Stability, and the Scale Length for Energy Deposition*

Several of the conclusions at which we shall arrive on the basis of the quasi-static model depend critically on certain assumptions, in addition to those regarding the boundary conditions. In this section we discuss these assumptions and their consequences in detail. In several cases we are led to conclusions radically different from those of Rosner, Tucker, and Vaiana (1978).

We assume that the loop is geometrically symmetric about the vertical plane through the dipole (perpendicular to the plane of Fig. 2) and, furthermore, that the energy input as a function of s is symmetric about this plane. Rosner, Tucker, and Vaiana also state that they assume symmetry about the top of the loop, but do not distinguish between geometrical symmetry and symmetry of energy input. However, from their later discussion it is evident that symmetry in both these senses is meant. They further state that this assumption can be made without loss of generality. We question this latter statement, since their conclusion that the temperature maximum must occur at the top (or apex) of the loop, and the chain of reasoning that follows, depend directly on it. Their argument depends on the disappearance of the conductive flux at the apex of the loop, which requires a maximum or minimum in the temperature, $T(s)$, at this point. Generally, in a geometrically symmetrical loop this can come about only if the energy input is also symmetric. An asymmetric input will displace the temperature maximum from the apex, which will thus (in the constant-area, gravity-free case) have no special properties.

If a symmetrical energy input is assumed, it is still not necessary for the temperature maximum to appear at the top of the loop [$S(T_{\max}) = S_{\max}$ in the notation of Rosner, Tucker, and Vaiana]. The energy input can have a maximum at some position on one side of the loop, in which case we expect that the temperature will also have a maximum at or near this position. Note that in order to maintain symmetry both the energy input and the temperature must have maxima at the corresponding positions on the other leg of the loop, and at the apex both will have a minimum. Thus, there will be zero conductive flux across the apex, and in the quasi-static case the portion of the loop between $S(T_{\max})$ and $S_{\max}$ loses energy by radiation only. Rosner *et al.* argue that this portion of the loop must

be thermally unstable because it does not cool by conduction; however, their conclusion is incorrect. By this reasoning all quasi-static loop models in which the heat flux vanishes at the base, including those of Rosner *et al.*, should be unstable. These authors did not realize that, even though the heat flux vanishes at two points, conduction may still be important in the intervening region. For example, in their models, the form of the temperature profile depends critically on conduction, even though the conductive flux vanishes at the base and at the apex. In addition, conduction will clearly be important in determining the response of the loop to a perturbation. Hence there is no reason to expect, *a priori*, that models with a temperature maximum at the apex are more stable than those with maxima at the sides.

The response of a quasi-static loop to a fluctuation in the energy input requires detailed time-dependent calculations which we are at present investigating. Two kinds of fluctuation in the energy input may be considered. If the energy input changes permanently (whether symmetrically or asymmetrically with respect to the apex), then the loop will adjust by adopting a new quasi-static configuration. Mass flow will occur, and the densities, temperatures, temperature gradients, and possibly the position of $T_{\max}$ will change until the whole loop, including the region at the top, is once again in energy balance. In the case of a perturbation in the energy input whose time average is zero, an analysis of the growth rate of the resulting temperature perturbations must be made before questions of stability can be answered. If the wavelength is sufficiently short, such perturbations will be damped by conduction regardless of whether or not there is conduction across the surfaces at the apex of the loop and $S(T_{\max})$. However, it should be noted that under transient conditions, i.e., temporary departures from the quasi-static configuration, the temperature extremes at these points need not be maintained.

Thus from the discussion above we conclude that the temperature maximum need not necessarily occur at the loop apex. The contention of Rosner, Tucker, and Vaiana (1978) that the scale length for energy deposition is small must also be disputed, since it is based on the conclusion regarding the position of the temperature maximum.

III. COMPUTATIONAL METHOD

To compute solutions for our loop model, we consider an initial value problem governed by the momentum and energy equations (4) and (5) above and subject to boundary conditions at the base of the loop ($s = s_b$) and a symmetry condition at the apex ($s = s_a$). We assume that $T = 3 \times 10^4$ K is the level at which the conductive flux vanishes (see § II*b*). A shooting technique is then employed to adjust the plasma number density $n(s = s_b)$ at the base such that the temperature gradient vanishes at the apex of the loop. Note that the boundary condition at the apex is not essential and is due solely to our assumption that the loop is symmetric about the apex (§ II$_b$). This convenience permits us to obtain solutions using only half the loop. The complete boundary condition is that at $s = \pm s_b$, $T = 3 \times 10^4$ K, and $dT/ds = 0$, where $-s_b$ is the position of the other base of the loop. Nonsymmetric solutions can be obtained by integrating over the whole loop and using this boundary condition.

It is convenient to reformulate the momentum and energy equations (4) and (5) as three, first-order, ordinary differential equations with temperature T, electron number density n, and conductive flux F_c as the dependent variables, and distance s along the loop from the dipole origin as the independent variable. The resulting equations are

$$\frac{dT}{ds} = -F_c/(A\alpha T^{5/2}), \tag{14}$$

$$\frac{dn}{ds} = \frac{n}{T}\left(\frac{mg_{\parallel}}{2k} + \frac{F_c}{A\alpha T^{5/2}}\right), \tag{15}$$

$$\frac{dF_c}{ds} = A[\epsilon - n^2\Lambda(T)], \tag{16}$$

where $A(s)$ is the cross-sectional area of the loop, $\alpha T^{5/2}$ is the thermal conductivity coefficient, m is the proton mass, k is Boltzmann's constant, $g_{\parallel}(s)$ is the acceleration of solar gravity along the loop, $\Lambda(T)$ is the radiative loss function, $\epsilon(s)$ is the energy input per unit volume—cgs units are used throughout. For the case of a line dipole $A(s) = A(s = s_a)\sin^2\phi$ where $\phi = s/h$ is the angle between the local horizontal plane at the dipole origin and a line from the dipole origin to the point s (see Fig. 2). The thermal conductivity coefficient is taken to be $\alpha T^{5/2}$, where $\alpha \approx 10^{-6}$ in cgs units (see Spitzer 1962, pp. 143–147). For our single fluid description of a fully ionized plasma, the fluid mass density is taken to be nm where m is the proton mass.

The radiative loss function $\Lambda(T)$ (in ergs s^{-1} cm^3) is based on the calculations of Raymond, Cox, and Smith (1976) as modified by Raymond 1976 (private communications) for a solar plasma with abundances given by Allen (1973). Cooling by excitation of neutral hydrogen and cooling by argon are included. Forbidden-line cooling below 10^6 K is removed to make the calculations more appropriate to the solar transition region. Raymond's calculations were fitted by power laws of the form $\Lambda(T) = \Lambda_0(T/T_0)^m$ over eight temperature ranges between 10^4 and 10^8 K. Table 1 lists

TABLE 1

POWER-LAW APPROXIMATIONS [$\Lambda(T) = \Lambda_0(T/T_0)^m$] TO THE RADIATIVE LOSS FUNCTION

T_0	Λ_0	m
1.00×10^4	9.31×10^{-24}	+7.17
1.56×10^4	2.26×10^{-22}	−0.839
3.16×10^4	1.25×10^{-22}	+1.43
1.00×10^5	6.46×10^{-22}	−0.0307
2.51×10^5	6.28×10^{-22}	−1.74
6.31×10^5	1.26×10^{-22}	−0.0792
2.00×10^6	1.15×10^{-22}	−0.664
3.16×10^7	1.84×10^{-23}	+0.293

the values of Λ_0, T_0, and m for each temperature range. The lower boundary of a given power law approximation is just T_0.

The numerical integration of equations (14), (15), and (16) upward along the loop is accomplished using a computer code devised by Shampine and Gordon (1975). The code is basically a variable order of interpolation, variable step size formulation of classic Adams methods. The stepping procedure is subject to a local error criterion containing both relative and absolute error terms. For our purposes a relative error of 10^{-4} and absolute error of unity have proved to be quite sufficient in controlling the global error, i.e., the error at the apex of the loop upon completion of the integration. The reader is referred to Shampine and Gordon (1975) for further details.

The shooting technique referred to above is simply a systematic method of varying the initial value of the density n_b at the loop bottom ($s = s_b$) in order to obtain a solution such that the temperature gradient vanishes at the loop apex. The iterative procedure used is based on Newton's method for finding zeros of polynomials. One assumes that the temperature gradient at the loop apex is some unknown function of the base density n_b, call it $g_t(n_b)$. Two guesses for n_b enable one to estimate dg_t/dn_b, and this slope is then used to make the next estimate for n_b, etc. Provision is made for inflection points in the curve g_t as suggested by Hamming (1973, chap. 4). Beginning with a reasonably good initial guess ($\pm$ a factor of 5), the procedure usually brings $|g_t|$ to less than 10^{-7} of the maximum dT/ds along the loop within 10 iterations.

The differential emission measure $\xi(T)$ is computed according to the definition of Craig and Brown (1976). For present purposes, this definition yields

$$\xi[T(s)] = A(s)n^2(s)/|dT/ds| \, . \qquad (17)$$

It is evident that $\xi(T) \to \infty$ at the base and apex of the loop as well as any other points where the temperature gradient vanishes. However, these singularities are integrable, as is required by observations.

IV. RESULTS

Figures 3 through 6 show sample results obtained from the numerical model described above. For these examples we take the energy deposition ϵ to be constant, i.e., uniformly distributed over the loop volume. The uniform distribution allows comparison with the analytical treatments of Craig, McClymont, and Underwood (1978) and Rosner, Tucker, and Vaiana (1978). Other cases in which ϵ is nonuniformly distributed, e.g., $\epsilon = f(T)$, $f(n)$, or $f(B)$, shall be investigated and reported in subsequent publications.

In Figure 3 we show results for a typical loop of length $l = 10^{10}$ cm and area factor $\Gamma = 2$. The energy input $\epsilon = 5 \times 10^{-4}$ ergs cm^{-3} s^{-1}, so that the total energy deposited in half the loop is $\sim 2 \times 10^{23}$ ergs s^{-1}. Consider a cylindrical volume element having a width $\delta s = 1$ cm along the magnetic field line defining the loop and an area $A(s)$ determined by the loop geometry as discussed in §§ II and III above (see Fig. 2). For this case $A(s = s_a)$, the apex area, is 10^{17} cm^2. Figure 3 shows the power flowing into such a volume element

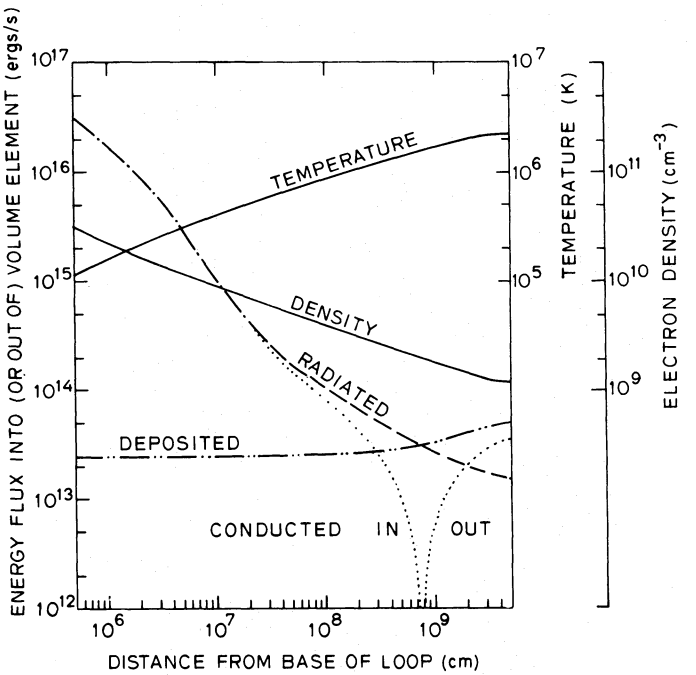

FIG. 3.—Energy flux deposited into, radiated out of, and conducted into (or out of) a cylindrical-shaped volume element with its axis along the axis of the coronal loop and a thickness $\delta s = 1$ cm along the axis of the loop (see Fig. 2). The loop length $l = 10^{10}$ cm and the area factor $\Gamma = 2$. Energy is deposited uniformly at a rate $\epsilon = 5 \times 10^{-4}$ ergs cm^{-3} s^{-1} over the loop volume of 4.09×10^{26} cm^3. The cross-sectional area at the loop apex $A_a = 10^{17}$ cm^2.

by mechanical energy deposition (and possibly conduction) and the balancing power flowing out by radiation (and possibly conduction). It is interesting to note that for $T \lesssim 10^6$ K the energy deposition ϵ is unimportant, and hence radiative losses are balanced by conductive transport. Thus we see that energy deposition near the bottom of the loop could be some two orders of magnitude higher without affecting the temperature or density structure of the loop. Further, we see that for $T \gtrsim 1.5 \times 10^6$ K energy deposition is greater than radiative loss, and thus conductive losses are required to maintain energy balance. As discussed in § II*b*, we find that approximately half the energy deposited in the loop is radiated away in the coronal portion of the loop. Hence the bulk of the deposited energy is not conducted down to the transition region, as is sometimes suggested.

Figure 4 gives further examples of model results, again for uniform energy deposition and a typical loop length of $l = 10^{10}$ cm. The variations of n and T along the loop are shown for two values of the energy input ϵ (10^{-4} and 10^{-3} ergs cm^{-3} s^{-1}) and two values of Γ (2 and 50). The model should be valid down to a temperature at which the optical depth of the material significantly affects the radiative losses: hence the curves have been plotted down to temperatures $\sim 10^5$ K.

In Figure 4 we see that a change in ϵ changes both the temperature and density. This is to be expected, since equation (13) indicates that the loop temperature and density are not independent. Note, however, that if we drop the boundary condition (that the heat flux vanish at the base), then the density no longer need increase with increasing ϵ. Of course, the temperature must still increase with increasing ϵ because a rise in energy input demands a rise in the conductive heat flux, which in turn requires a higher temperature.

Figures 4 and 5 show that increases in the energy input ϵ cause general increases in both temperature T and number density n as well as $\xi(T)$. We note that an order-of-magnitude change in ϵ causes only about a factor 2 change in T, but about a factor 5 change in n. Since radiated power is proportional to n^2 and more weakly dependent on T, we see that variations in energy input to a loop result in similar variations in radiated energy output (loop brightness as observed in EUV or X-rays), but that variations in loop temperature should be small. Observational experience at X-ray wavelengths apparently bears out this conclusion, in that loop brightness varies considerably over the Sun, whereas active region temperatures determined from X-ray observations are generally confined to a small range around 2 to 3 $\times 10^6$ K.

The effect of a changed loop geometry (parametrized here by Γ) on $n(s)$ and $T(s)$ is less marked. Along a loop of given length l and cross-sectional area at the apex A_a, an increase in Γ from 2 to 50 results in about a factor of two increase in n (Fig. 4). The temperature gradient along the loop drops generally and the apex temperature decreases slightly. The decrease in apex temperature appears surprising when we note that the effect of a variable area is to add an extra term of the form $[d(T^{7/2})/ds](d \ln A/ds)$ to the right-hand side of the heat equation (3). Since this term is nonnegative, it represents an extra heat source. However, we note that for $10^5 \lesssim T \lesssim 3 \times 10^7$ K the radiative loss function $\Lambda(T)$ is inversely related to T (see Table 1). Hence the lower temperature at the apex (for $\Gamma = 50$) actually serves to increase the radiative losses and help balance the additional heat source induced by the increase in Γ.

Although n and T turn out to be relatively insensitive to Γ, the differential emission measure $\xi(T)$ is quite significantly affected (Fig. 5). The measure $\xi(T)$, defined in equation (17), is plotted in Figure 5 for $l = 10^{10}$ cm, $A_a = 1$ cm^2, and the same ϵ and Γ values as Figure 4. Thus in Figure 5 we see that an increase in Γ results in relatively larger amounts of

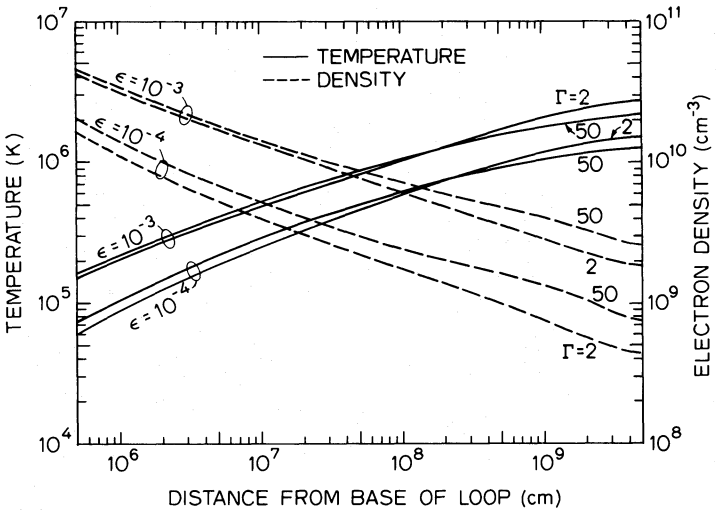

FIG. 4.—Variation of temperature T (*solid lines*) and electron density n (*dashed lines*) for a loop of length $l = 10^{10}$ cm. Curves are shown for uniform energy inputs ϵ of 10^{-3} and 10^{-4} ergs cm^{-3} s^{-1} and area factors Γ of 2 and 50. Note that n is a stronger function of ϵ or Γ than is T.

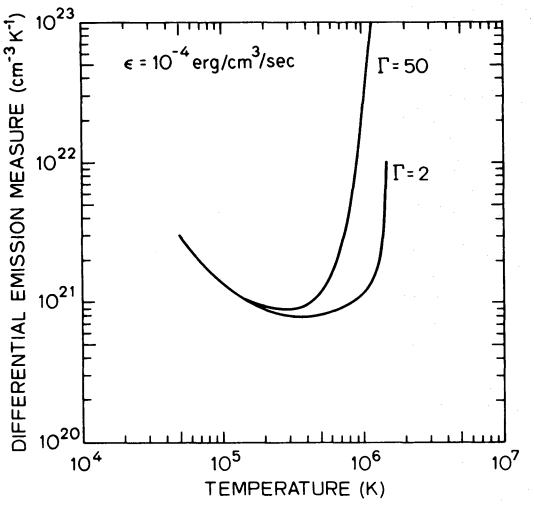

FIG. 5a

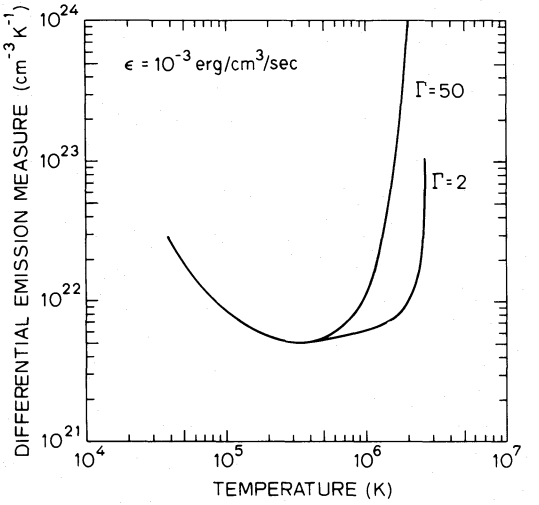

FIG. 5b

FIG. 5.—Differential emission measure with respect to temperature $\xi(T)$ for a loop of length $l = 10^{10}$ cm, apex cross-sectional area = 1 cm^2, and area factors Γ of 2 and 50. The $\Gamma = 50$ curve has been multiplied by a constant factor [16.6 in (*a*); 21.1 in (*b*)] in each case to normalize it to the $\Gamma = 2$ curve at low T. The energy input to the loop is uniform at values of (*a*) 10^{-4} and (*b*) 10^{-3} ergs cm^{-3} s^{-1}. Note the minimum in $\xi(T)$ at $T \sim 3$ to 5×10^5 K. The power-law (*straight line*) portion of the $\xi(T)$ curve at $T \sim 0.5$–2×10^6 K which is evident for $\Gamma = 2$ and $\epsilon = 10^{-3}$ disappears for larger Γ or lower ϵ.

material at coronal temperatures ($\sim 10^6$ K) relative to the material at transition region temperatures ($\sim 10^5$ K).

With our numerical model we can also test the order-of-magnitude equality between the radiative and conductive heat losses that was derived from the boundary conditions (see § II*b*). Letting n_0 and T_0 be the electron density and temperature at the loop apex and L be the size scale of the corona, equation (13) becomes:

$$Ln_0^2\Lambda(T_0) = \alpha \frac{T_0^{7/2}}{L}, \tag{18}$$

so that

$$\Lambda(T_0) = \lambda T_0^{\beta}, \tag{19}$$

$$T_0^{7/2-\beta} = \frac{\lambda}{\alpha}(n_0 L)^2. \tag{20}$$

Thus the relation is dependent on the form assumed for the radiative losses, i.e., β. (Rosner *et al.* assumed that $\lambda = 10^{-18.8}$ and $\beta = -\frac{1}{2}$, which, when substituted into eq. [20], leads directly to their eq. [4.3]; Craig *et al.* assumed $\beta = -1$, which leads to their eq. [41].)

It should be noted that the length L appearing in equation (20) is not necessarily the same as the loop length l. If the temperature is sufficiently low and the loop height large, then the relevant size scale for the corona becomes the gravitational scale height, i.e.,

$$L = \frac{2kT}{mg}. \tag{21}$$

However, for most solar loops the parameters are such that the loop length is much less than the gravitational scale height; hence, $L \approx l$.

In Figures 6*a* and 6*b*, $n_0 l$ is plotted against T_0 for several cases, where n_0 and T_0 are the density and temperature at the loop apex. The energy input ϵ is 10^{-4} and 10^{-3} ergs cm^{-3} s^{-1} in Figures 6*a* and 6*b*, respectively. We also plot the approximate formulae based on equation (20) that were derived by Rosner *et al.* and Craig *et al.* For a given l and T_0 the approximate formulae predict the value of n_0 well within an order of magnitude for values of Γ up to 50, at least. Thus equation (20) may be considered a useful and reliable formula for almost all cases of interest and approximation (13) is justified. Note, however, that in Figure 6*a* the exact result begin to deviate from the approximate formula at large L. This is due to gravity. For $T = 3 \times 10^6$ K, the gravitational scale height is $\sim 5 \times 10^{10}$ cm, which is comparable to the loop length, $l = 3 \times 10^{10}$ cm.

V. CONCLUSIONS

1) X-ray images of coronal loops (Fig. 1) indicate significant variations of loop cross-sectional area along the loop length, i.e., area factor $\Gamma > 1$ (see Fig. 2). Numerical modeling of coronal loops with $\Gamma > 1$ shows Γ to be a significant factor in the determination of a loop's temperature and density structure (Fig. 4) and an especially important factor in the determination of the differential emission measure $\xi(T)$ which characterizes a loop's UV and X-ray spectrum (Fig. 5).

2) Along loops of a given length l and apex cross-sectional area A_a, an upward variation of Γ causes a general rise in electron density, but a general fall in temperature gradient (Fig. 4). These changes prove to have a cumulative effect on $\xi(T)$ leading to large increases in ξ for T near T_{max} (Fig. 5). Hence we conclude that, other factors aside, increased values of

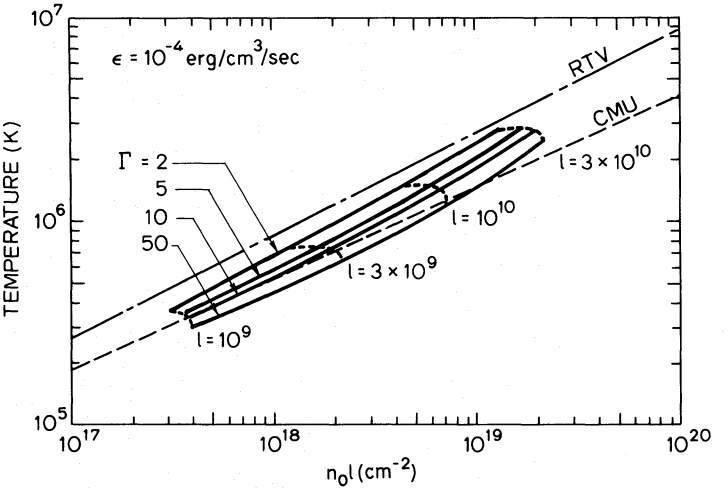

FIG. 6a

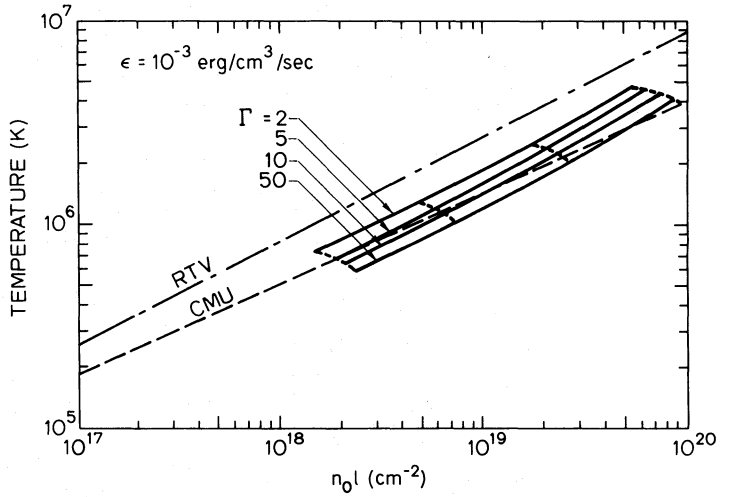

FIG. 6b

FIG. 6.—Variation of loop apex temperature T_0 with ($n_0 l$), apex electron density times loop length. Curves are shown for four values of Γ and the dashed curves are for constant values of l. The energy input is uniform at values of (*a*) 10^{-4} and (*b*) 10^{-3} ergs cm^{-3} s^{-1}. The analytical models of Rosner, Tucker, and Vaiana (RTV) and Craig, McClymont, and Underwood (CMU) are shown for comparison. These power-law relations stem from the assumption that conductive and radiative energy transport are equal and from a power-law approximation to the radiative loss function.

Γ lead to larger amounts of plasma at coronal temperatures relative to that at transition region temperatures.

3) For model loops with Γ significantly greater than unity the form for $\xi(T)$ is significantly different from that of analytical models (compare Fig. 5 above and Fig. 11 of Rosner, Tucker, and Vaiana 1978). So it seems prudent to use numerical modeling when making detailed analyses of UV and X-ray spectral observations of coronal loops.

4) Based on order-of-magnitude equality between radiative and conductive heat losses, both Rosner, Tucker, and Vaiana (1978) and Craig, McClymont, and Underwood (1978) derive analytical relations between temperature and electron density at the loop apex and loop scale length (eq. [20] above). We have compared these relations with our numerical model results for loops with Γ = 2 to 50 and conclude that the analytical relations are quite useful, being no more than a factor of 2 or 3 away from the numerical results.

5) Rosner, Tucker, and Vaiana (1978) argue that for a loop symmetrical about the apex the temperature maximum must occur at the apex. We point out that a symmetrical displacement of temperature maxima away from the loop apex does not, per se, make the top of the loop unstable, and thus conclude that even a symmetrical loop may have T_{max} away from the apex.

A real coronal active region will normally be composed of many loops, each having its own length, area factor, and possibly energy input. The details of an

observationally determined emission measure curve for a complete active region will result as much from the *distribution* of these parameters as from the physical processes occurring in an individual loop. Thus it is important to establish, both theoretically and observationally, how this distribution is related to factors such as the state of evolution of the region, its structure, and the topology of the magnetic field. The spectroscopic study of many individual loops in the extreme-ultraviolet and X-ray regions would appear to be a profitable way to attack this problem.

The authors thank Ian Craig of Glasgow University and Joshua Knight of Stanford University for useful advice during the course of this work and Irene Stratton for help with the manuscript. The reviewer's helpful criticism also made a substantial contribution to the final result. This work also benefited from the authors' participation in the Third *Skylab* Workshop on Active Regions. We gratefully acknowledge financial support from the National Aeronautics and Space Administration under contract NAS8-32263 and grant NGL-05-020-014.

REFERENCES

Allen, C. W. 1973, *Astrophysical Quantities* (3d ed.; London: Athlone).
Antiochos, S. K. 1976, Stanford University Institute for Plasma Research, Rept. No. 679.
Antiochos, S. K., and Krall, K. R. 1979, *Ap. J.*, **229**, 788.
Antiochos, S. K., and Sturrock, P. A. 1976, *Solar Phys.*, **49**, 359.
———. 1978, *Ap. J.*, **220**, 1137.
Brueckner, G. E., and Bartoe, J.-D. F. 1978, *Bull. AAS*, **10**, 416.
Craig, I. J. D., and Brown, J. C. 1976, *Astr. Ap.*, **49**, 239.
Craig, I. J. D., McClymont, A. N., and Underwood, J. H. 1978, *Astr. Ap.*, **70**, 1.
Gerassimenko, M., Solodyna, C. V., and Nolte, J. T. 1978, *Solar Phys.*, **57**, 103.
Hamming, R. W. 1973, *Numerical Methods for Scientists and Engineers* (New York: McGraw-Hill).
Nicolas, K. R., Brueckner, G. E., Tousey, R., Tripp, D. A., White, O. R., and Athay, R. G. 1977, *Solar Phys.*, **55**, 305.
Pneuman, G. W., and Kopp, R. A. 1978, *Solar Phys.* **57**, 49.
Pye, J. P., Evans, K. D., Hutcheon, R. J., Gerassimenko, M., Davis, J. M., Krieger, A. S., and Vesecky, J. F. 1978, *Astr. Ap.*, **65**, 123.
Raymond, J. C., Cox, D. P., and Smith, B. W. 1976, *Ap. J.*, **204**, 290.
Rosner, R., Tucker, W. H., and Vaiana, G. S. 1978, *Ap. J.*, **220**, 643.
Sandlin, G. D., Brueckner, G. E., and Tousey, R. 1977, *Ap. J.*, **214**, 898.
Shampine, L. F., and Gordon, M. K. 1975, *Computer Solution of Ordinary Differential Equations* (San Francisco: Freeman).
Spitzer, L. 1962, *Physics of Fully Ionized Gases* (New York: Wiley), chap. 5.
Underwood, J. H., *et al.* 1974, *Prog. Astr. Aeronaut.*, **48**, 161.
Vaiana, G. S., Davis, J. M., Giacconi, R., Krieger, A. S., Silk, J. S., Timothy, A. F., and Zombeck, M. 1973, *Ap. J.*, **185**, 147.

SPIRO K. ANTIOCHOS and JAMES H. UNDERWOOD: Institute for Plasma Research, Stanford University, Stanford, CA 94305

JOHN F. VESECKY: Center for Radar Astronomy, Stanford University, Stanford, CA 94305